COMMUNICATIONS IN SCIENCE AND TECHNOLOGY
Homepage: cst.kipmi.or.id

Maximizing oil recovery in sandstone reservoirs through optimized ASP injection using the super learner algorithm

Dike Fitriansyah Putra[a,b,e,*], Mohd Zaidi Jaafar[b], Ku Muhd Na'im Khalif[c], Apri Siswanto[d], Ichsan Lukman[e], Ahmad Kurniawan[a,e]

[a]*Department of Petroleum Engineering, Universitas Islam Riau, Pekanbaru 28284, Indonesia*
[b]*Faculty of Chemical and Energy Engineering, Universiti Teknologi Malaysia, Skudai 81310, Malaysia.*
[c]*Centre for Mathematical Sciences, Universiti Malaysia Pahang Al-Sultan Abdullah, lebuh Persiaran Tun Khalil Yaakob, Kuantan 26300, Malaysia*
[d]*Departement of Informatics Engineering, Universitas Islam Riau, Pekanbaru 28284, Indonesia*
[e]*Center of Energy Studies, Universitas Islam Riau, Pekanbaru 28284, Indonesia*

Article history:
Received: 27 January 2025 / Received in revised form: 8 June 2025 / Accepted: 13 June 2025

Abstract

Optimizing the Alkaline-Surfactant-Polymer (ASP) injection process remains a persistent challenge in Enhanced Oil Recovery (EOR), particularly in heterogeneous sandstone reservoirs where traditional reservoir simulators are constrained by high computational demands and limited flexibility. This study introduces a novel application of the Super Learner (SL) ensemble, a stacking-based machine learning algorithm integrating multiple base models (XGBoost, SVR, BRR, and Decision Tree), to systematically predict and optimize ASP injection parameters. Unlike previous approaches, our method blends high-fidelity CMOST simulation data with machine learning precision in which it enables real-time optimization with field-scale relevance. Using 500 simulation scenarios validated by laboratory input, the SL model achieved exceptional predictive performance (R^2 = 0.988, RMSE = 0.304), outperforming all individual learners. The optimal recovery factor (RF) of 79.49% was obtained with the finely tuned concentrations of surfactant (5483.29 ppm), polymer (2242.61 ppm), SO_4^{2-} (5610.15 ppm), CO_3^{2-} (7053.59 ppm), and Na^+ (9939.35 ppm). Remarkably, the SL approach could reduce optimization time from 10 hours (CMOST) to under 1 minute; this underscored its potential for real-time operational deployment. The novelty of this work lies in its integrated use of ensemble learning to capture the complex and non-linear interactions between ionic chemistry and oil mobilization behavior, offering a field-ready AI framework for rapid and adaptive EOR design. This approach paves the way for the intelligent optimization of ASP schemes by minimizing the reliance on computationally intensive simulations while ensuring chemical and economic efficiency in marginal or complex reservoirs.

Keywords: EOR, ASP; oil recovery; machine learning; super leaner

1. Introduction

Alkaline, Surfactant, Polymer (ASP) injection is widely recognized as one of the most effective techniques in Chemical Enhanced Oil Recovery (EOR)[1,2,3,4]. This method leverages the synergistic effects of alkalis, surfactants, and polymers to significantly enhance oil recovery. The role of alkali component is crucial as it increases the pH of the injected fluid, thereby reducing surfactant adsorption and generating in-situ surfactants in acidic crude oil conditions [5,6]. This process, in turn, leads to a greater reduction in interfacial tension (IFT) and alters wettability, making the oil more mobilizable. Surfactants further decrease the IFT between crude oil and the injected fluids, enabling any trapped oil droplets to flow with greater ease. In contrast, polymers increase the viscosity of the injected fluid, which improves the mobility ratio between the displacing water and reservoir oil; this then leads to more uniform sweep efficiency and reduced channeling.

Sandstone reservoirs, known for their diverse mineral composition, provide favorable conditions for ASP injection due to their relatively low adsorption of anionic (negatively charged) compounds [7,8,9].

However, implementing ASP injection at the field scale can pose several challenges, including high chemical costs, operational complexity, and uncertainties in terms of reservoir conditions [7,10,11]. It is therefore deemed essential to design an ASP injection scheme that can effectively balance maximizing recovery with minimizing costs and complexities.

Traditionally, conventional reservoirs simulation models have been utilized to optimize ASP injection with the Recovery Factor (RF) used as the primary decision variable [1,2,10,12]. These conventional models, however, encounter significant limitations when applied to the complex and large-scale nature of EOR datasets. They often require extensive computational

* Corresponding author. Tel.: +62-812-9874-4099
Email: dikefp@eng.uir.ac.id
https://doi.org/10.21924/cst.10.1.2025.1649

resources, are time-consuming, and introduce various uncertainties [10,12]. To address these challenges, Artificial Intelligence (AI) and Machine Learning (ML) techniques have emerged as effective alternatives for the optimization of EOR processes. Compared to traditional approaches, AI-driven methods excel in processing large datasets, identifying intricate non-linear relationships, and significantly reducing uncertainties [13,14,15,16].

To make it clearer, Support Vector Machines (SVM) and Multi-Layer Perceptron Neural Networks (MLP-NN) have been effectively utilized to predict the efficiency of polymer flooding and surfactant-polymer flooding. These methods have demonstrated a strong alignment with field data, facilitating the precise optimization of injection strategies [17,18]. Furthermore, Least Squares Support Vector Machine (LSSVM) models, when paired with Genetic Algorithms (GA) for optimization, have shown remarkable accuracy in predicting RF and Net Present Value (NPV), and they could achieve correlation coefficients (R^2) greater than 0.993 [13,19]. These studies underscore the advantage of machine learning models in capturing complex, multi-dimensional, and non-linear interactions among critical EOR parameters, which seem be difficult to be achieved by traditional methods.

Building on these advancements, ensemble learning techniques have garnered interest for their ability to enhance model robustness by aggregating the predictions of multiple models. Super Learner (SL), a stacking-based ensemble method, combines various machine learning algorithms to reduce biases, minimize variance, and improve prediction accuracy[20,21]. In the realm of petroleum engineering, it has proven to be highly effective, surpassing individual models in predicting any essential reservoir properties, such as dead oil viscosity and water saturation [22,23].

This study utilized the SL ensemble to optimize the ASP injection process with three main objectives: (1) to optimize critical ASP parameters, including sulfate ions (SO_4^{2-}) from surfactants, sodium ions and carbonate ions (Na^+, CO_3^{2-}) from alkali sources, and polymer concentrations [2,9], thereby maximizing the RF; (2) to compare the performance of the SL model against traditional models such as Bayesian Ridge, Support Vector Regression (SVR), and XGBoost, thereby demonstrating the effectiveness of ensemble learning; and (3) to identify the optimal conditions for minimizing IFT and enhancing sweep efficiency, which can have practical applications in real-world field operations.

By integrating laboratory-scale data, and simulation model data with advanced ML techniques, this study presents a novel framework aimed at bridging the gap between experimental and field-scale optimization of ASP injection, ultimately contributing to improved and more efficient oil recovery.

2. Materials and Methods

2.1. Experimental setup

2.1.1. Data collection

The study commenced with the creation of a Cartesian reservoir model specifically designed to simulate the behavior of oil reservoirs during ASP injection. This model represented the reservoir as a grid of cells to facilitate a detailed analysis of fluid dynamics and chemical interactions [2,9,24]. Multiple scenarios were executed using the model to explore various combinations of injection parameters, resulting in a diverse dataset. The collected data then underwent processing to ensure consistency, reliability, and noise reduction; this ultimately yielded a high-quality dataset suitable for machine learning applications.

To determine the most significant factors determining oil recovery, feature selection techniques were employed. The following features were identified as the ones with the greatest impact on oil recovery: the concentrations of each chemical component crucial to modify rock wettability, reduce IFT, and enhance sweep efficiency. Salinity plays a significant role in the effectiveness of surfactants by affecting micelle stability and surfactant solubility, which, in turn, influences IFT reduction. IFT is a direct measure of the interaction forces between the oil and the injected water phases; lower IFT values indicate improved conditions for oil mobilization, making it a key parameter in evaluating the success of the ASP injection process.

The selected features served as the inputs for training various machine learning models with the target variable being oil RF. These trained models aimed to predict the effectiveness of different ASP injection scenarios, thereby providing valuable insights in the optimization of recovery processes.

2.1.2. Machine learning model and super learner ensemble

To capture the complex relationships between ASP injection parameters and RF, a range of machine learning models was utilized. Each algorithm offered a distinct approach to understand the interplay between parameters:

1) Bayesian Ridge Regression (BRR): This probabilistic model adjusts the regularization strength automatically based on training data, making it robust against multicollinearity and able to provide confidence intervals for predictions. Here, it serves as a baseline to understand linear trends and parameter uncertainty in the dataset [14].
2) SVR is well-suited to capture non-linear relationships between features and RF. By utilizing different kernel functions, it effectively handles high-dimensional data and provides precise predictions for the complex non-linear dependencies inherent in ASP injection optimization.
3) Linear Regression (LR) and Decision Tree Regresses (DTR): These models serve as baseline models for comparison purposes. LR helps to identify any significant linear relationships between the features, while the DTR provides interpretability in identifying parameter splits and interactions. The Decision Tree model highlights how parameters, such as chemical concentration, affect RF at different thresholds.
4) eXtreme Gradient Boosting (XGBoost) Regressor: XGBoost is a highly regarded gradient boosting algorithm recognized for its accuracy, efficiency, and capability to capture complex non-linear interactions among variables. It employs an ensemble of decision trees to predict RF to effectively address overfitting through regularization techniques while considering the effects of various injection scenarios.

To enhance predictive performance, the Super Learning (SL) Ensemble was utilized, leveraging the strengths of individual models. The SL method, an ensemble stacking technique, combines predictions from multiple base learners to reduce bias and variance, purposely to produce more accurate and generalized outcomes. K-fold cross-validation was employed to train the SL ensemble to minimize overfitting and ensure robustness. By integrating multiple models, the SL ensemble capitalized on their individual strengths that resulted in improved overall predictive accuracy. The evaluation metrics used to assess each model's performance included the Coefficient of Determination (R^2) to measure how well predictions align with actual results, and Root Mean Square Error (RMSE) to quantify the magnitude of prediction errors.

2.1.3. Parameter optimization and sensitivity analysis

The SL model was utilized to forecast the RF by examining various combinations of ASP component concentrations and salinity levels. The optimization process employed a grid search technique, which systematically evaluated different parameter configurations to identify the combination that produced the highest RF. This approach facilitated an efficient exploration of the solution space, ensuring the selection of the most effective injection strategy.

Additionally, a sensitivity analysis was conducted to assess the relative impact of each parameter on RF. This analysis yielded valuable insights into the most influential factors, enabling targeted adjustments to enhance the effectiveness of ASP injection. The results revealed that certain parameters, particularly polymer concentration and salinity, had a significant impact on RF, underscoring the necessity for their precise management to maximize recovery.

2.1.4. Model calibration and validation

To validate the reliability of the model, results from the SL were compared with both experimental and simulation data. The close correlation between model predictions and experimental outcomes confirmed the SL model's accuracy in capturing the intricate relationships between injection parameters and RF. Cross-validation was employed to further ensure the model's robustness to provide a statistical measure of its generalizability across diverse datasets.

The model's hyperparameters were iteratively refined to enhance prediction performance. A number of adjustments were made to the learning rate, regularization strength, and other critical hyperparameters to achieve an optimal balance between accuracy and control overfitting. The final calibrated model was subsequently utilized to simulate various ASP injection scenarios, producing the predictions of optimal recovery and offering insights into the effective use of chemicals, alongside economic considerations. These predictions underscored the potential to significantly improve recovery rates, while minimizing chemical costs and maximizing operational efficiency.

2.2. Equations

2.2.1. Data processing

The research was based on secondary data from [25] establishing a base case that featured a sandstone reservoir characterized by a relatively tight rock distribution and low salinity. From the analysis of the reservoir properties, as presented in Fig. 1, it was evident that the reservoir rock exhibited a tendency toward water wettability with the intersection of the relative permeability curves for water and oil occurred at a water saturation of 0.52. Table 1 shows that the oil had a gravity value of 25°API (American Petroleum Institute), classifying it as heavy-medium oil.

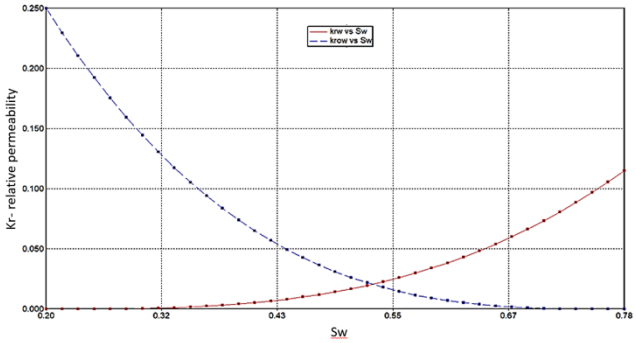

Fig. 1. Correlation of the relative permeability

Table 1. Reservoir rock properties data [25,26]

Parameter	Value	Unit
Oil Gravity	25	°API
Gas Oil Ratio	250	SCF/stb
Bubble Point Pressure	350	psi
Salinity	20000	ppm
μo at Initial Pressure	0.82	cp
Reservoir Temperature	173	°C
Reservoir Depth	5400-5512	ft
Reservoir Pressure	1615	psi
Rock Compressibility	1.39×10^{-5}	psi^{-1}
Formation Volume Factor	1.105	Bbl/stb

2.2.2. Hydrocarbon components

The oil was sourced from the Central Sumatra Basin field with hydrocarbons characterized by a high C7+ content. Table 2 presents the mole percentage values of each hydrocarbon component used in this study.

2.2.3. Reservoir model

The model was based on a Cartesian grid conceptual framework featuring a heterogeneous distribution of rock types. Although it consisted of five layers, as presented in Table 3, it effectively simulated the layering observed in the field with the dimensions of 1,000 ft in length and 200 ft in width. Fig. 2 depicts the 3D grid distribution with depths in the range of 5,400 to 5,512 ft, porosity values between 0.15 and 0.3, and permeability spanning from 100 to 300 md [25,26]. Table 4 presents the field initialization with an Original Oil In Place (OOIP) estimate of 0.49 MMbbl.

Fig. 2 displays a three-dimensional permeability model of a reservoir that illustrates the spatial distribution of permeability

values within a specific section of the reservoir as of January 1, 2021. The model employed a color-coded scheme to represent various permeability ranges, offering essential insights into the reservoir's flow characteristics. Segmented into distinct blocks, each block was assigned a color that corresponded to its permeability. The legend on the right side of the figure detailed the permeability values associated with each hue.

Table 2. Hydrocarbon components

Components	Concentration mole (Mole%)
H_2S	0
CO_2	0.3783
N_2	0.4645
CH_4	11.2789
C_2H_6	0.1622
C_3H_8	0.2503
i-C_4H_{10}	0.1832
n-C_4H_{10}	0.4448
i-C_5H_{12}	2.3216
n-C_5H_{12}	2.6256
C_6H_{14}	13.2666
C_7H_{16}	68.6240

Table 3. Model grid properties

Grid Properties	Description
Grid Type	Cartesian
Layers Count	5
Total Block	50
Width	200 ft
Length	1000 ft

Table 4. Initial reservoir volume

Parameter	Value
Original Oil in Place	0.491 MMbbl
Gross Formation Volume	28 MMSCF
Formation Pore Volume	6.442 MMSCF

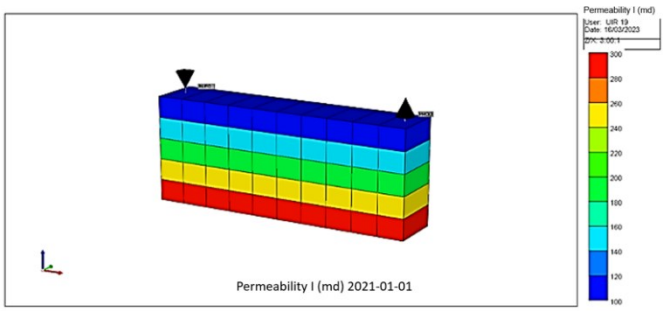

Fig. 2. Cartesian cross section model (permeability)

The model revealed a layered distribution of permeability with the lower layers predominantly displaying blue and cyan tones (indicative of lower permeability values), while the upper layers exhibited red and orangish shades (denoting higher permeability). This suggests the presence of a heterogeneous reservoir, characterized by vertical variations in permeability that may result from differing rock types or varying depositional environments. The differing colors and permeability values across the model signified that the reservoir's heterogeneity stems from variations in rock properties such as grain size, sorting, and cementation, all of which influence porosity and permeability.

Notably, the existence of distinct high-permeability zones (highlighted in red) and low-permeability zones (shown in blue) indicated that fluid flow within the reservoir was likely to be non-uniform, potentially presenting challenges for efficient sweep during fluid injection for EOR.

The black arrows positioned atop certain blocks indicated the probable points of injection or production. These may represent injection wells, where fluid is pumped into the reservoir to displace oil, or production wells, where oil is extracted. The strategic placement of these arrows in the higher permeability regions is likely intentional as higher permeability facilitates more efficient fluid flow and aids in maintaining reservoir pressure.

2.2.4. Base case initialization

The initial fractional composition of the sandstone reservoir comprised 80% Barite and 20% Kaolinite. Table 5 outlines the chemical composition of the ASP base case, detailing the specific elements used in its formulation.

Table 5. ASP composition [27]

Parameter	Value (ppm)
Alkaline (Na_2CO_3)	10,000
Surfactant (Base + SO_4^{2-})	15,000
Polymer (Base)	2,000

The production history of the reservoir extends over five years from 2020 to 2025, initially relying on primary recovery methods. In 2025, an ASP injection strategy is implemented, which continues for one year until 2026.

Following the ASP injection phase, operations transition to waterflooding by 2026. This waterflooding phase acts as a post-chemical injection flushing mechanism, designed to mobilize and recover any residual oil that has been displaced by the chemical process.

This integrated approach combines the enhanced mobilization capabilities of ASP injection with the flushing efficiency of waterflooding, all aimed at maximizing oil recovery from the sandstone reservoir throughout the operational period.

Fig. 3 illustrates the relationship between salinity (ppm) and IFT (dyne/cm) for various surfactant concentrations, comparing laboratory data with model simulations. It highlights the critical role of salinity and surfactant concentration in minimizing IFT for EOR.

The optimal combination was a 0.05% surfactant concentration at 20,500 ppm salinity, achieving the lowest IFT (10^{-3} dyne/cm), necessary for mobilizing trapped oil. The IFT rose to 102 after water injection but dropped to the critical level of 10^{-3} under optimal conditions. The close match between lab and model results confirmed the model's reliability for field implementation planning.

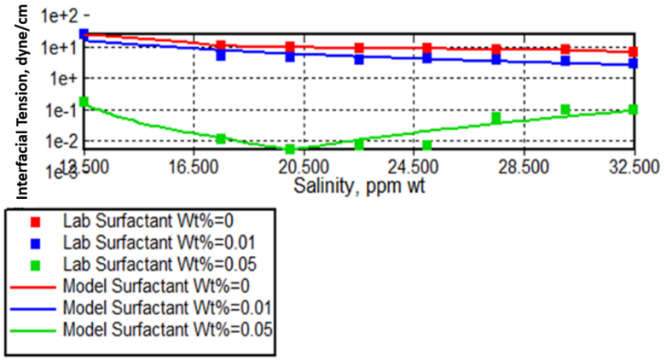

Fig. 3. Salinity variation and IFT base case (CMG)

Table 6. Ionic parameter (sun et al. 2016)

Variable Name	Codes/Symbol	Min	Max
SO_4^{2-} (ppm)	INJ_SO4	2500	10000
Na^+ (ppm)	INJ_Na	2500	10000
CO_3^{-2} (ppm)	INJ_CO3	2500	10000
Surfactant (ppm)	INJ_SFT	2500	10000
Polymer (ppm)	INJ_Polymer	500	2500

Table 5 presents five parameters, complete with their respective minimum and maximum values, which define the input range for model evaluation. These parameters are essential for determining whether the model meets performance standards.

The RMSE serves as a crucial metric for assessing model performance as it quantifies the standard deviation of prediction errors, the discrepancies between predicted and actual values. A lower RMSE indicates superior model accuracy. The formula is:

$$RMSE = \sqrt{\frac{\sum_{i=1}^{n}(y_i - \hat{y}_i)^2}{n}} \quad (1)$$

The coefficient of determination (R^2) is the criterion for usage. It represents the adjacent of the dependent value to the best-fitting regression line. It is written as:

$$R^2 = 1 + \frac{\sum(y_i - \hat{y}_i)^2}{\sum(y_i - \bar{y}_i)^2} \quad (2)$$

In addition to a high R^2 value, a low error indicates good model performance. The R^2 score ranges from nil to one; getting closer to one means that the data model matches the actual data.

2.2.5. Super leaner method

The Enhanced Super Learner (SL) is an ensemble learning model, which is distinct from deep learning models. It achieves superior accuracy by synthesizing predictions from multiple algorithms through comprehensive cross-validation. The key points are that the SL consolidates outputs from four foundational machine learning algorithms to enhance predictive accuracy, which employs cross-validation to ensure robust model performance across various datasets, and basic machine learning algorithms serve as the core foundation that assesses the relationship between measured and predicted values for ASP injection using cross plots for each dataset. Then, by integrating multiple algorithms and utilizing cross-validation, the SL minimizes errors and improves prediction reliability, particularly in ASP injection modeling. This approach is optimal for achieving precision in predictions without the computational demands of deep learning models.

The study focuses on optimizing ASP injection and predicting RF values for EOR in sandstone reservoirs, highlighting the advantages of artificial intelligence, specifically the SL algorithm, over traditional simulation methods.

Key findings included that AI-driven approaches exhibited a distinct advantage over conventional simulators when it came to modeling complex interactions and optimizing ASP parameters. The SL algorithm delivered greater accuracy and faster computational speeds, especially when combined with CMG reservoir simulation software. Secondly, Four foundational algorithms were employed to model the non-linear interactions of ASP consisting of SVM that effectively managed non-linear relationships in high-dimensional datasets, XGB that exceled in capturing intricate interactions among parameters, Bayesian Framework that provided a means to manage uncertainties and offered probabilistic insights, and Decision Tree (DT) that ensured simplicity and interpretability in the analysis of feature interactions.

The advantage of the SL Algorithm integrated the strengths of the aforementioned base models, producing a robust and accurate predictive tool for optimizing RF. It significantly reduced computational time compared to traditional simulation techniques. The last one was the analysis concentrated on the injection concentrations of surfactant, polymer, SO_4^{2-}, CO_3^{2-}, and Na^+. These parameters played some crucial roles in altering wettability, reducing interfacial tension, and controlling mobility, all of which were essential for the success of ASP injection.

3. Results and Discussion

3.1. Base model simulation

A total of 1,038 simulations were conducted using CMG CMOST to produce a comprehensive set of results. From these simulations, a representative dataset of 500 samples was randomly and evenly selected to ensure a diverse and unbiased representation of the parameter space. The RF values observed in this dataset ranged from 66.94% to 80.56%, highlighting the varying efficiency of different ASP injection parameter combinations. The highest RF of 80.56% was achieved with the

following injection parameters: surfactant concentration of 8,500 ppm, polymer concentration of 2,300 ppm, SO_4^{2-} at 2,500 ppm, CO_3^{2-} at 4,000 ppm, and Na^+ at 10000 ppm. These specific values represented an optimal configuration for maximizing oil recovery within the reservoir.

The observed behavior indicated a correlation between the dynamics of ion concentrations and oil production rates. Notably, when the gmol values of these ions increased, oil production rates significantly rose, suggesting that these ions positively contributed to improve sweep efficiency, reduce interfacial tension, or enhance the chemical effectiveness of the ASP solution. Conversely, when the gmol values decreased, the oil production rate continued to rise, albeit at a more consistent and stable rate. This implied that while the presence of these ions is essential, their impact becomes less pronounced beyond a certain threshold.

This phenomenon can be attributed to several factors. The initial increase in ion concentration might enhance wettability alteration and reduce IFT, thereby facilitating the improved mobilization of residual oil. However, once the chemical interactions reach an optimal level, the system attains a balance, and further changes in ion concentration yield diminishing returns in oil recovery. This highlights the importance of meticulously managing the injection strategy to sustain optimal ion concentrations for maximum efficiency.

Overall, these findings emphasize the significant role that chemical interactions and ion exchange play in the success of ASP injection. Gaining a deeper understanding of the interplay between injection parameters and reservoir chemistry offers valuable insights for optimizing the recovery process, ensuring that every component of the chemical mixture is utilized to its fullest potential for effective and economical enhancement of oil production.

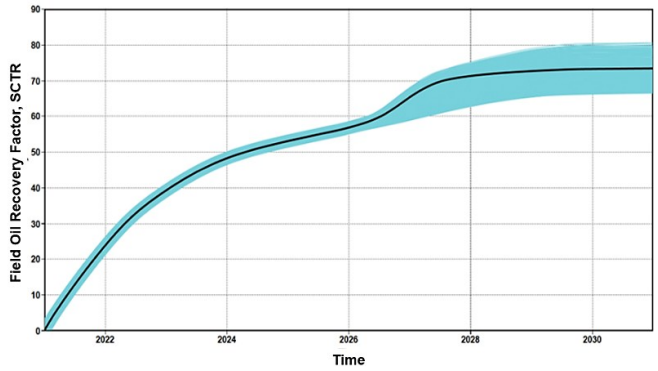

Fig. 4. Field oil recovery factor over time

Fig. 4 illustrates the RF over time. The black line depicts the increase in RF relative to the base case, while the blue one represents the RF growth from various experimental data sets. The overall shape of the curve, which transitions from an initial rise to a plateau, demonstrated the typical performance of an ASP injection process: the initial mobilization of trapped oil was followed by a peak in efficiency, culminating in a stabilization of recovery. This trend served as a valuable illustration of both the short-term and long-term effects of EOR techniques on reservoir performance. The pronounced rise followed by a plateau aided the authors to understand the anticipated yield and plan further interventions if needed. A significant increase following the initiation of ASP injection on January 1, 2025, suggested that the five parameters had a substantial impact on the RF enhancement.

Fig. 5 through 9 depict the concentration profiles of several key parameters, highlighting their dynamic changes over time. Notably, the concentrations of SO_4^{2-}, Na^+, and CO_3^{2-} displayed distinct increasing and decreasing patterns, reflective of ongoing ion exchange and interactions between the ASP and the reservoir. These ion exchanges were pivotal in modifying the chemical environment of the reservoir, which, in turn, determined the efficiency of oil displacement and recovery.

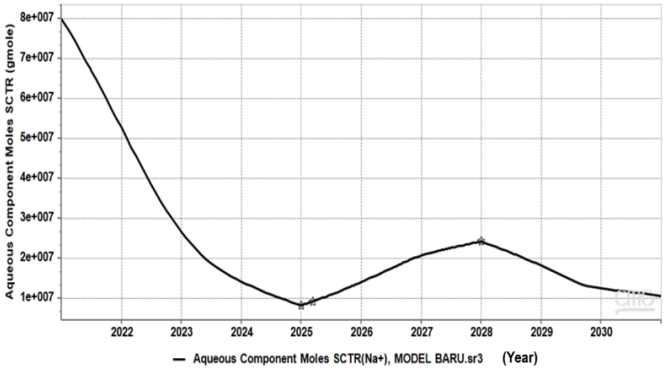

Fig. 5. Concentration profile of Na^+

Fig. 5 illustrates the dynamic behavior of Na^+ concentration throughout the study period. Initially, in 2020, the Na^+ concentration was approximately 8e+007 gmole (or 20,000 ppm). However, it saw a significant decrease, dropping to below 1e+007 gmole by 2025. This decline reflected various interactions with the reservoir, including adsorption, wettability alteration, and the formation of in-situ surfactants.

By 2025, Na^+ concentration is predicted to be stable at its lowest level, indicating an equilibrium between chemical reactions and the availability of ions. From 2026 to 2029, the concentration of Na^+ is predicted to again increase from 9e+006 to 2.5e+007 gmole (or 2250 to 6250 ppm). This rise is likely attributable to ASP injection or ion desorption. The observed peaks and troughs during this period highlight the ongoing exchanges of ions and the impact of secondary injections that support EOR processes.

After 2029, Na^+ concentration is projected to decline gradually, indicating a stabilization phase and diminishing efficiency of ASP, marking a transition toward equilibrium and reduced incremental recovery. This fluctuation illustrates the complex interplay between injected chemicals, reservoir rocks, and fluids during ASP processes.

Fig. 6 illustrates the concentration of sulfate ions (SO_4^{2-}) in the reservoir. From 2022 to 2025, sulfate levels remained consistently low, suggesting that there were no significant ASP components present prior to injection.

However, started from 2025, there will be a sharp increase in sulfate concentration, reaching a peak around 2028. This rise indicates active sulfate injection, which enhances oil mobilization by reducing IFT, altering wettability, and generating in-situ surfactants through reactions with alkali and crude oil acids.

Following 2028, sulfate levels will begin to decline, likely due to interactions with reservoir rocks, fluid depletion, or

decreased injection rates. This decline signifies a shift towards stability, reflecting diminishing returns as the more accessible zones have already been impacted. This trend underscores the progression toward equilibrium in the EOR process.

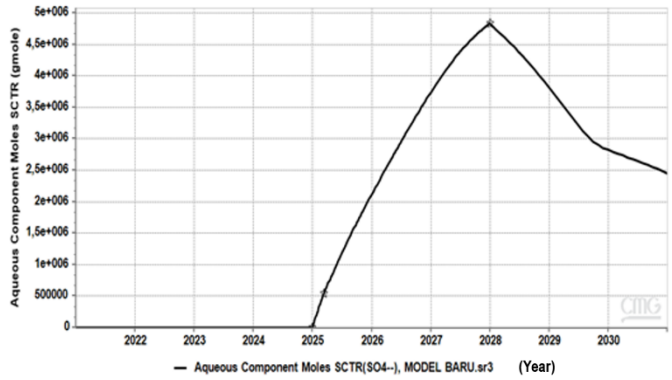

Fig. 6. Concentration profile of SO_4^{2-}

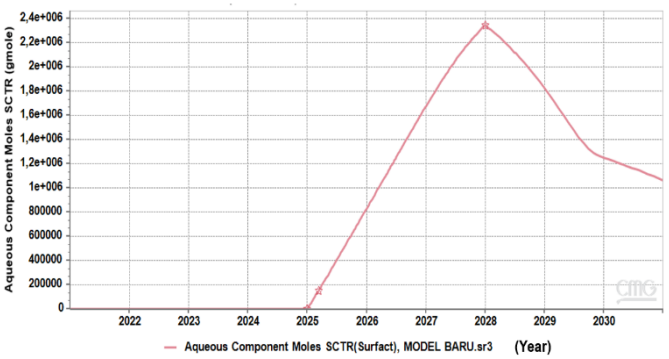

Fig. 7. Concentration profile of Surfactant

Fig. 7 illustrates the dynamics of surfactant concentration within the reservoir. From 2022 to 2025, the concentrations remained close to zero, indicating a lack of significant injection during this period. By 2025, surfactant injection commences with concentrations peaking around 2028. This peak signifies optimal IFT reduction and the maximum effectiveness of oil mobilization.

Following 2028, surfactant levels begin to decline, likely due to adsorption onto reservoir rocks, depletion from various reactions, or a transition to a different EOR phase, such as water flooding. This decline suggests diminishing returns from further injection and a move toward equilibrium.

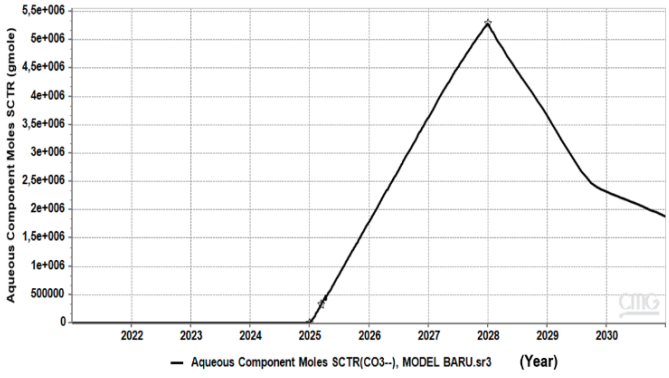

Fig. 8. Concentration profile of CO_3^{2-}

From 2022 to 2025, as illustrated in Fig. 8, carbonate ions (CO_3^{2-}) remained at negligible levels, indicating a lack of active injection. However, by 2025, carbonate concentrations rise sharply, and reach a peak by 2028. This increase is attributed to the reactions between injected alkali (such as Na_2CO_3) and naturally occurring acids, which enhance pH control and improve surfactant effectiveness by reducing IFT.

The peak observed by 2028 represents an optimal carbonate activity, leading to improved oil recovery through alterations in wettability and a reduction in surfactant adsorption. Following this peak, carbonate levels gradually decline as a result of consumption in reactions (such as the formation of $CaCO_3$ precipitates) or reduced injection rates, marking a transition to equilibrium and diminishing returns.

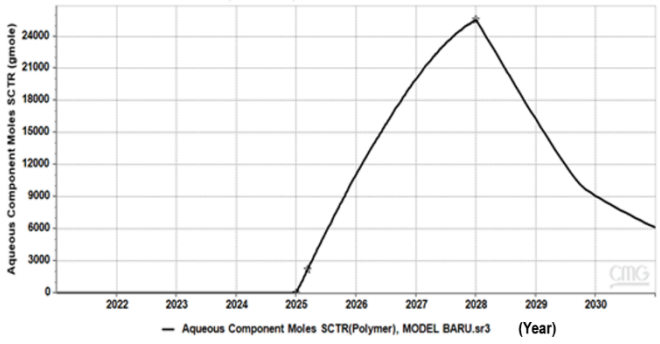

Fig. 9. Concentration profile of polymer+

From 2022 to 2025, polymer concentration remained close to zero, indicating that no injection occurred during this period (see Fig. 9). Beginning by 2025, polymer levels increase significantly, reaching a peak by 2028. This peak signifies an optimal polymer injection, enhancing viscosity to improve sweep efficiency and minimize fingering.

Following 2028, polymer concentration begins to decline due to degradation, consumption, or reduced injection rates. This decline indicates a transition to a maintenance phase that relies on the previously established effects for ongoing oil recovery.

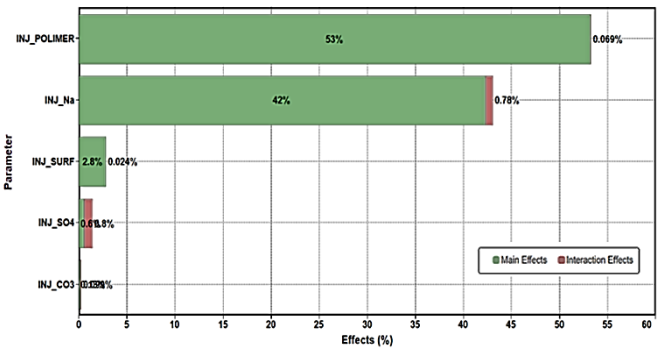

Fig. 10. Five key parameters of ASP injection

Fig. 10 illustrates the contributions of various injection parameters to the RF. The green bars indicate the direct effects, while the red ones denote the interaction effects.

Of the major parameters, Polymer played a crucial role, accounting for 53% of the contribution. It significantly enhanced viscosity and sweep efficiency, exhibiting minimal

interaction effects at 0.069%, thereby functioning predominantly in isolation. Sodium, contributing 42%, was vital for altering wettability and improving surfactant performance, displaying a higher interaction effect of 0.78%. This suggests a synergistic relationship with other components, such as surfactants.

Turning to the minor parameters, the Surfactant contributed only 2.8%, proven effective in reducing IFT, but its impact was limited due to already optimized wettability conditions. Sulphate (-0.18%) and Carbonate (-0.05%) demonstrated negligible or even negative effects, likely caused by precipitation or scaling issues, which necessitate careful management to prevent impeding recovery.

Given that Polymer and Sodium largely operated independently, optimizing each parameter individually could be highly effective. By prioritizing Polymer and Sodium, we could maximize the RF while minimizing reliance on less impactful elements like Sulphate and Carbonate. It was crucial to avoid the excessive use of surfactants and to properly manage Sulphate and Carbonate as their mismanagement might diminish efficiency. This highlights the importance of balanced injection strategies.

Table 7. Five parameters of ASP flooding optimization

Ranking	Features	Effect
1	INJ_Polymer	0.5306
2	INJ_Na	0.4278
3	INJ_Surf	0.0280
4	INJ_SO4	0.0068
5	INJ_CO3	0.0001

Fig. 10 and Table 7 examine the influence of five parameters on the RF based on 500 CMOST simulation runs. Polymer (Impact: 0.5306) became the most influential parameter, enhancing viscosity and sweep efficiency, which helped to prevent channeling and ensured uniform oil displacement. This was critical for mobility control during ASP injection. Ionic Na^+ (Impact: 0.4278) ranked as the second most important factor, as it optimized salinity to reduce IFT and maximize surfactant efficiency, thereby significantly improving oil mobilization.

Surfactant (Impact: 0.0280) had a limited effect, likely due to already optimized wettability, suggesting that further additions may yield diminishing returns. Both Ionic SO_4^{2-} (Impact: 0.0068) and CO_3^{2-} (Impact: 0.0001) showed minimal impact, indicating their limited role in altering wettability or facilitating chemical interactions, which helped to mitigate risks such as scaling or inefficiencies.

3.2. Super learner ensemble

Fig. 11 illustrates the correlation among various injection components and the RF. Each cell in the matrix displays the correlation coefficient between two parameters with the values in the range of -1 to +1. A positive correlation indicates that as one variable increases, other is likely to increase as well, whereas a negative correlation suggests that as one variable rises, other tends to decrease. The color bar on the right reflects the strength of the correlation.

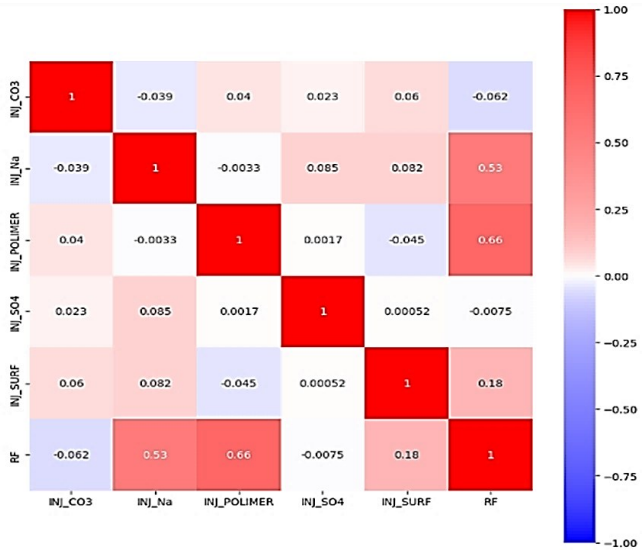

Fig. 11. Mathematical correlation of parameters

Polymer (0.66) exhibited a strong positive correlation with RF, emphasizing its significant role in enhancing sweep efficiency and mobilizing oil. While, Sodium (0.53) showed a moderately strong correlation, highlighting its importance in optimizing salinity, reducing IFT, and improving surfactant efficiency. Surfactant (0.18) demonstrated a weak correlation, suggesting that its efficacy largely depended on the contributions from both polymer and sodium. CO_3^{2-} (-0.062) displayed a weak negative correlation, which may indicate potential challenges such as precipitation or scaling. SO_4^{2-} (-0.0075) had a negligible negative correlation, suggesting minimal or slight adverse effects on RF.

The interactions between polymer and sodium (0.085) revealed a weak synergy, where sodium's effect on wettability alterations complemented the viscosity effect of polymer but functioned mostly independently. The relationship between sodium and surfactant (0.082) also showed a weak interaction, indicating that sodium optimized pH levels for surfactant activity though its amplifying effects were found limited. In contrast, the negative correlation between polymer and surfactant (-0.045) suggests that the increased levels of polymer may reduce the concentration or impact required for surfactant effectiveness.

Overall, the dominance of polymer and sodium demonstrated the strongest positive correlations with RF, underscoring their critical roles in viscosity control and salinity optimization. To achieve maximum efficiency, it was focused on polymer and sodium while managing carbonate and sulphate levels to mitigate negative impacts such as scaling. Nevertheless, most of parameters operated independently with limited synergy, which simplified the optimization process for EOR design.

3.3. Key driver of oil recovery

Of the five key parameters affecting RF, INJ_POLYMER became the primary factor. It had the most significant impact, enhancing sweep efficiency by increasing the viscosity of the

injected fluid. INJ_Na was also essential, playing a vital role in altering wettability and optimizing surfactant activity.

In contrast, the effects of INJ_CO3 and INJ_SO4 were found minimal, characterized by weak or negative correlations. These parameters provided little to no benefit and may even impede recovery, necessitating their limited use.

There was an interdependency between INJ_Na and INJ_POLYMER that demonstrated slight synergy; however, it was more critical to optimize each parameter individually. The benefits of surfactant injection showed limited reliance on these interactions, reinforcing the importance of independent optimization.

The SL algorithm featured a predictive model built using ASP injection parameters as the input and RF as the output. Multiple base learners were trained and evaluated based on R^2 (prediction accuracy) and RMSE (error magnitude). The most effective learners were then integrated into the SL ensemble to enhance the accuracy of RF predictions.

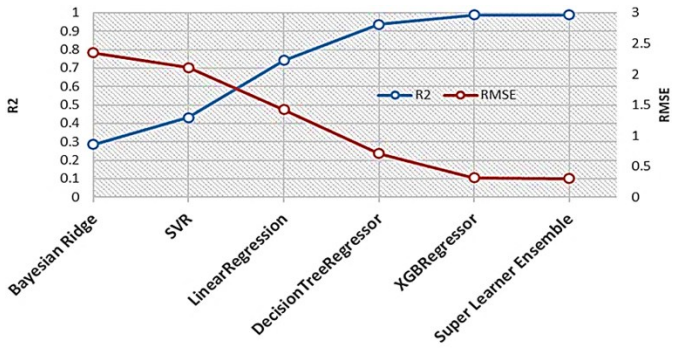

Fig. 12. Comparison of R^2 and RMSE for Each Learner

Fig. 12 illustrates the performance of several machine learning models—Bayesian Ridge, SVR, Linear Regression, Decision Tree Regressor, XGBoost Regressor, and the Super Learner Ensemble (SLE), using an EOR dataset. It provides a comparison of R^2 and RMSE for each model. These metrics are crucial for assessing the predictive capacity of each model, with R^2 representing the proportion of variance accounted for by the model and RMSE indicating the average magnitude of the prediction errors.

In the figure, R^2 is depicted by the blue line, while RMSE is represented by the red one. A higher R^2 value suggests greater model accuracy, reflecting how well the predicted values correspond to the actual values. Conversely, a lower RMSE value signifies better performance, as it indicates that the average error in predictions is small.

The model comparison revealed that Bayesian Ridge achieved an R^2 of approximately 0.9 and an RMSE of around 3. This relatively high R^2 value (~0.9) indicated that the model captured a significant portion of the variability in the data. However, the RMSE was notably high at around 3, suggesting considerable prediction errors. Despite explaining a large fraction of the variance, these high prediction errors implied that the model may be prone to overfitting or may struggle to effectively manage complex non-linear relationships.

SVR demonstrated an R^2 value of approximately 0.7 and a RMSE of about 2.5. Although SVR had a lower R^2 than Bayesian Ridge, indicating it accounted for less variance in the data, its RMSE was slightly better, suggesting it managed prediction errors more effectively. SVR may excel at capturing non-linear relationships, which could lead to reduced error rates despite its lower R^2. However, there is a concern that it may struggle to fully capture the complexities of the dataset.

Linear Regression showed a moderate performance with an R^2 around 0.5 and an RMSE of approximately 2. This model explained about half of the variance in the data, indicating that it struggled with non-linear patterns. The RMSE value hinted at limited effectiveness in minimizing prediction errors, making Linear Regression less suitable for more intricate datasets.

The Decision Tree Regressor had an R^2 of approximately 0.3 and an RMSE of around 1.5. This model's lower R^2 indicated that it captured relatively little variance in the data. However, the RMSE suggested that it had lower prediction errors compared to other models discussed. The combination of a low R^2 and a relatively lower RMSE implied that the Decision Tree may be overfitting to specific data points, resulting in a model that performed well in certain cases but lacked overall reliability across the dataset.

In contrast, XGBoost Regressor exhibited a high R^2 value of approximately 0.95 and a significantly lowered RMSE of about 0.75. This indicated that XGBoost explained nearly all the variance in the data while maintaining minimal prediction errors. Utilizing a boosted decision tree approach, XGBoost effectively captured complex patterns, making it the most accurate model among those evaluated. Its high R^2 and low RMSE positioned it as an optimal choice for complex EOR predictions.

The SLE achieved an R^2 of approximately 1 and an RMSE of around 0.1, making it the top-performing model. This indicated that the ensemble effectively explained nearly all the variance in the data and had an exceptionally low average prediction error. By combining the strengths of multiple models, the SLE created a robust predictor that captured both linear and non-linear relationships while addressing complexities that individual models might overlook. This demonstrated the power of ensembling, as it leveraged the advantages of various algorithms for superior performance.

In Fig. 12, the SLE model exhibited the highest performance of all the base learner models, achieving an R^2 value of 0.988. This indicated a near-perfect fit between the predicted and actual data, reflecting the model's excellent capability to capture complex non-linear relationships between the input parameters and the resultant RF values. Additionally, the SLE model recorded the lowest RMSE of 0.304, indicating that it made the most accurate predictions with minimal error compared to other models.

Using the SLE model, the prediction of the optimal RF value was conducted by inputting the minimum and maximum values of the injection parameters, including surfactant, polymer, SO_4, CO_3^{2-}, and Na^+ concentrations. This approach allowed for a comprehensive evaluation of potential outcomes, ultimately helping in identifying the parameter configuration that maximized RF. The SLE model's high R^2 and low RMSE values highlighted its reliability and precision in optimizing ASP injection scenarios, providing valuable insights for EOR.

For optimization using the SLE algorithm, as illustrated in Fig. 4, 500 new datasets were randomly generated with the maximum and minimum parameter values adjusted to align with

the original range utilized for generating datasets in CMOST. This methodology facilitated a thorough exploration of potential scenarios to identify the optimal parameters for ASP injection. Following the optimization, as displayed in Fig. 6, the RF was determined to be 79.49% with the following corresponding injection parameters: surfactants at 5483.29 ppm, polymers at 2242.61 ppm, SO_4^- at 5610.15 ppm, CO_3^{2-} at 7053.59 ppm, and Na^+ at 9939.35 ppm.

The optimization process was also implemented using Python programming, achieving the highest RF value of 79.49% in less than one minute of computational time. In contrast, the CMOST software required approximately 10 hours to generate and optimize the Design of Experiments (DoE), ultimately arriving at the RF value of 80.65%. This stark difference in computational time underscores the efficiency of machine learning approaches, such as the SL algorithm, for rapid optimization.

The findings suggest that, under comparable reservoir conditions, researchers and engineers are able to leverage machine learning models to predict RF values much more swiftly by directly inputting the optimized parameters. This enhanced optimization capability not only saves time but also allows for increased iterations, thereby improving decision-making processes and the feasibility of ASP injection projects.

As for the SLE, it stood out as the best model, achieving the highest R^2 value of 0.988 and the lowest RMSE of 0.304. It effectively captured complex non-linear interactions in ASP injection. By integrating multiple learners, the ensemble mitigated biases and variances, making it the most dependable predictor for RF optimization.

XGBoost, as the Premier Individual Model, stood out among individual models, achieving a high R^2 of approximately 0.95 and a low RMSE of roughly 0.75. It exceled in managing non-linear EOR data although it did not match the precision of the ensemble approach.

Insights into key parameters: (1) Polymer (2242.61 ppm) was the most influential factor as it enhanced sweep efficiency by improving viscosity and regulating fluid mobility. (2) Na^+ (9939.35 ppm) was found essential for altering wettability, optimizing surfactant efficiency, and pH balance. (3) Surfactant (5483.29 ppm) was effective in reducing IFT, thereby mobilizing trapped oil. (4) CO_3^{2-} (7053.59 ppm) facilitated pH control and promoted the formation of HCO_3^-, enhancing wettability and the performance of surfactants. (5)SO_4^{2-} (5610.15 ppm) stabilized chemical mixtures, contributing to IFT reduction.

Ionic Interactions and Chemical Dynamics showed that the generation of HCO_3^- ions through the reactions of CO_3^{2-} played a crucial role in pH adjustment, minimizing surfactant adsorption, and producing in-situ surfactants that improved reservoir wettability and efficiency.

Practical Applications displayed efficiency and scalability in which the SLE optimized ASP injection with remarkable speed, achieving RF of 79.49% under a minute, compared to CMOST's lengthy 10-hour process. Its accuracy and rapid execution enabled effective field-scale adaptation.

The SLE exceled in predicting and optimizing RF, underscoring the vital contributions of polymer and Na^+ in augmenting ASP efficiency. By integrating chemical insights with machine learning precision, this method guarantees high recovery rates, time efficiency, and scalability for real-world EOR applications. These findings highlight the significance of managing ionic interactions and utilizing advanced machine learning models to transform oil recovery strategies.

4. Conclusion

This study confirms that the SL ensemble algorithm is a powerful and efficient tool for optimizing ASP injection in sandstone reservoirs. By integrating the predictive strengths of multiple base models, which are XGBoost, SVR, Bayesian Ridge, and Decision Tree, the SL model achieved near-perfect predictive accuracy (R^2 = 0.988) and minimized prediction error (RMSE = 0.304), significantly outperforming traditional simulators such as CMOST and individual machine learning algorithms. Notably, the SL model identified an optimal ASP configuration resulting in the RF of 79.49%, all while reducing optimization time from 10 hours to less than 1 minute, a leap forward in quantitative efficiency.

Mechanistically, the model uncovered that polymer and sodium ions became the primary contributors to recovery enhancement, accounting for over 95% of the total impact. Polymer concentration notably controlled mobility and sweep efficiency, while sodium ions regulated wettability and surfactant performance through salinity and pH adjustment. In contrast, surfactant, sulfate, and carbonate ions—though being essential for fine-tuning IFT and in-situ surfactant generation—exerted relatively minor or even adverse effects when used excessively, emphasizing the importance of precision dosing and balanced chemical interactions.

The practical field relevance of this work is underscored by the model's rapid execution and scalability. Its ability to perform real-time parameter optimization with high accuracy has made it suitable for dynamic reservoir management, field screening, or economic feasibility evaluations in both mature and marginal fields. By offering a data-driven, low-cost, and computationally light alternative to conventional ASP optimization workflows, this approach represents a significant advancement in modern EOR practices.

For future work, this framework can be expanded by incorporating economic metrics (e.g. NPV per chemical unit), real-time streaming field data, and uncertainty quantification techniques. Additionally, the inclusion of reactive transport modeling and integration with smart field operations (digital twin environments) will further strengthen its value as an intelligent decision-making tool for next-generation ASP projects.

Acknowledgements

The authors would like to express their sincere gratitude to the Center of Energy Studies (PSE) at Universitas Islam Riau (UIR), the Faculty of Chemical and Energy Engineering at Universiti Teknologi Malaysia (UTM), Johor, and Centre for Mathematical Sciences, Universiti Malaysia Pahang as well as Department of Informatics Engineering, UIR for their invaluable technical support throughout the course of this research. Finally, the authors also extend their thanks to the Directorate of Research and Community Service (DPPM) at Universitas Islam Riau for providing financial support under

contract number 1048/KONTRAK/P-MATCHING GRANT UMP-UIR/DPPM-UIR/10-2024, which was instrumental in making this study possible. Furthermore, special appreciation is given to the Petroleum Engineering Department at Universitas Islam Riau for their continuous administrative support, which facilitated the smooth progression of this research.

Glossary of Terms

Terms	Definition	Unit
ASP	Alkaline, Surfactant, Polymer	
EOR	Enhanced Oil Recovery	
RF	Recovery Factor	%
ML	Machine Learning	
IFT	Interfacial Tension	dynes/cm
AI	Artificial Intelligence	
SVM	Support Vector Machine	
MLP-NN	Multi-Layer Perceptron Neural Networks	
LSSVM	Least Squares Support Vector Machine	
GA	Genetic Algorithms	
NPV	Net Present Value	
R^2	Coefficients of Determination	
SL	Super Learner	
SLE	Super Learner Ensemble	
SVR	Support Vector Regression	
XGBoost	eXtreme Gradient Boosting	
BRR	Bayesian Ridge Regression	
RMSE	Root Mean Square Error	
API	American Petroleum Index	°API
DoE	Design of Experiments	
CMG	Computer Modelling Group	

References

1. D. F. Putra, M. Zaidi, R. I. Aldani, and R. Melysa, "Hybrid-alkali: A Synergy of Two Alkalis to Improve Efficiency of Alkali-Surfactant-Polymer (ASP) Flooding for the Oil Field," in *The 2nd International Conference on Design, Energy, Materials and Manufacture 2021 (ICDEMM 2021)*, Pekanbaru: AIP Conference Proceedings (2023).
2. A. M. Nasution and D. F. Putra, "Investigasi Sifat Ion Na(+) & NH4(+) Pada Hybrid-Alkali ASP Flooding Menggunakan Simulator CMG GEM 2020," *Lembaran Publikasi Minyak dan Gas Bum*, 56 (2022) 133–145.
3. C. Sun, H. Guo, Y. Li, G. Jiang, and R. Ma, *Alkali Effect on Alkali-Surfactant-Polymer (ASP) Flooding Enhanced Oil Recovery Performance: Two Large-Scale Field Tests Evidence*, J. Chem. (2020) 1–22.
4. H. Guo, G. Jiang, J. Zhang, J. Hou, K. Song, and Q. Song, *Alkali-surfactant-polymer ASP flooding field test using horizontal wells: Design, implementation and evaluation*, *in Proceedings - SPE Symposium on Improved Oil Recovery*, Tulsa Oklahoma: SPE, (2020) 1–15.
5. A. D. K. Wibowo, *Investigating potential application of bio-based polymeric surfactant using methyl ester from palm oil for chemical enhanced oil recovery (CEOR)*, Commun. Sci. Technol. 8 (2023) 235–242.
6. A. D. N'diaye, M. S. Kankou, B. Hammouti, A. B. D. Nandiyanto, D. F. Al Husaeni, *A review of biomaterial as an adsorbent: From the bibliometric literature review, the definition of dyes and adsorbent, the adsorption phenomena and isotherm models, factors affecting the adsorption process, to the use of typha species waste as a low-cost adsorbent*, Commun. Sci. Technol. 7 (2022) 140–153.
7. H. Zhong, T. Yang, H. Yin, J. Lu, K. Zhang, and C. Fu, *Role of Alkali type in chemical loss and ASP-flooding enhanced oil recovery in Sandstone formations*, in the SPE Annual Technical Conference and Exhibition, Dallas, Texas (2019) 431–445.
8. H. Zhong, T. Yang, H. Yin, C. Fu, and J. Lu, *The Role of Chemicals Loss in Sandstone Formation in ASP Flooding Enhanced Oil Recovery*, Dallas Texas (2018) 1–17.
9. D. F. Putra *et al.*, *Innovating EOR Strategies: Unlocking the Potential of Streaming Potential (Electrokinetic) as Sustainable and Ecofriendly Surveillance Tools for Monitoring ASP Fluid Front*, in The SPE Advances in Integrated Reservoir Modelling and Field Development Conference and Exhibition, Abu Dhabi, UAE, (2025) 1–13.
10. H. Guo, Y. Li, Y. Li, D. Kong, B. Li, and F. Wang, *Lessons learned from ASP flooding tests in China*, in The SPE Reservoir Characterisation and Simulation Conference and Exhibition, Abu Dhabi UAE (2017) 226–248.
11. H. Guo *et al.*, *ASP Flooding: Theory and Practice Progress in China*, J Chem, (2017) 1–11.
12. F. Abadli, *Simulation Study of Enhanced Oil Recovery by ASP (Alkaline, Surfactant and Polymer) Flooding for Norne Field C-segment,* Norwegian University of Science and Technology, (2012).
13. M. A. Ahmadi and M. Pournik, *A Predictive Model of Chemical Flooding for Enhanced Oil Recovery Purposes: Application of Least Square Support Vector Machine*, Petroleum, 2 (2016) 177–182.
14. D. Steineder, G. Vanegas, T. Clemens, and M. Zechner, *Deriving Alkali Polymer Parameter Distributions from Core Flooding by Applying Machine Learning in a Bayesian Framework to Simulate Incremental Oil Recovery*, in The 82nd EAGE Conference and Exhibition, Virtual: SPE, (2020) 1–21.
15. F. Hadavimoghaddam, M. Ostadhassan, M. A. Sadri, T. Bondarenko, I. Chebyshev, and M. Semnani, *Prediction of Water Saturation from Well Log Data by Machine Learning Algorithms: Boosting and Super Leaner*, J. Mar. Sci. Eng. 9 (2021) 1–23.
16. A. Larestani, S. P. Mousavi, F. Hadavimoghaddam, M. Ostadhassan, and A. Hemmati-Sarapardeh, *Predicting the Surfactant-Polymer Flooding Performance in Chemical Enhanced Oil Recovery: Cascade Neural Network and Gradient Boosting Decision Tree*, Alex. Eng. J. 61 (2022) 7715–7731.
17. M. M. Al-Dousari and A. A. Garrouch, *An Artificial Neural Network Model for Predicting the Recovery Performance of Surfactant Polymer Floods*, J. Pet. Sci. Eng. 109 (2013) 51–62.
18. L. Van Si and B. H. Chon, *Artificial Neural Network Model for Alkali-Surfactant-Polymer Flooding in Viscous Oil Reservoirs: Generation and Application*, Energies 9 (2016) 1–20.
19. J. Hou, Z. Guan Li, X. Long Ca, and X. Wang Song, *Integrating Genetic Algorithm and Support Vector Machine for Polymer Flooding Production Performance Prediction*, J. Pet. Sci. Eng., 68 (2009) 29–39.
20. E. C. Polley and M. J. Van Der Laan, *Super Learner In Prediction*, Berkeley, 266 (2010).
21. M. J. Van Der Laan, E. Polley, and A. Hubbard, *Super Leaner*, Berkeley, 222 (2007).
22. E. Khamehchi, M. R. Mahdiani, M. A. Amooie, and A. Hemmati Sarapardeh, *Modeling viscosity of light and intermediate dead oil systems using advanced computational frameworks and artificial neural networks*. J. Pet. Sci. Eng. 193 (2020) 107388.
23. F. Hadavimoghaddam *et al.*, *Prediction of Dead Oil Viscosity: Machine Learning vs. Classical Correlations*, Energies (Basel), 14 (2021) 1–6.
24. S. Munadi, Seismo-Electric Phenomena from Granite Containing Crude Oil, Science Contribution Oil and Gas, 30 (2007) 43–46.

25. A. Novriansyah, W. Bae, C. Park, A. K. Permadi, and S. S. Riswati, *Optimal Design of Alkaline – Surfactant – Polymer Flooding under Low Salinity Environment*, Polymers (Basel), 12 (2020) 1–11.
26. E. Effendi, R. Purwaningsih, Pujiarko, E. M. Adji, L. Notman, and J. Ewing, *Plan of Field Development of Tilan Field*, Pekanbaru, 2003.
27. Q. Sun, T. Ertekin, M. Zhang, and T. On, *A Comprehensive Techno-Economic Assessment of Alkali–Surfactant–Polymer Flooding Processes Using Data-Driven approaches,* Energy Reports, 7 (2021) 2681–2702.